ORIGINAL ARTICLE

JBMR®

^{18}F-NaF PET/CT IMAGING IN FIBROUS DYSPLASIA OF BONE

Georgios Z Papadakis,[1,2,3] Georgios C Manikis,[1] Apostolos H Karantanas,[1,3] Pablo Florenzano,[2,4] Ulas Bagci,[5] Kostas Marias,[1] Michael T Collins,[2] and Alison M Boyce[2]*

[1]Foundation for Research and Technology (FORTH), Institute of Computer Science (ICS), Heraklion, Greece
[2]Skeletal Disorders and Mineral Homeostasis Section, National Institute of Dental and Craniofacial Research (NIDCR), National Institutes of Health, Bethesda, MD, USA
[3]Department of Radiology, Medical School, University of Crete, Heraklion, Greece
[4]Endocrinology Department, Facultad de Medicina, Pontificia Universidad Catolica de Chile, Santiago, Chile
[5]Center for Research in Computer Vision, University of Central Florida, Orlando, FL, USA

ABSTRACT

Fibrous dysplasia (FD) is a mosaic skeletal disorder resulting in fractures, deformity, and functional impairment. Clinical evaluation has been limited by a lack of surrogate endpoints capable of quantitating disease activity. The purpose of this study was to investigate the utility of ^{18}F-NaF PET/CT imaging in quantifying disease activity in patients with FD. Fifteen consecutively evaluated subjects underwent whole-body ^{18}F-NaF PET/CT scans, and FD burden was assessed by quantifying FD-related ^{18}F-NaF activity. ^{18}F-NaF PET/CT parameters obtained included (i) SUV_{max} (standardized uptake value [SUV] of the FD lesion with the highest uptake); (ii) SUV_{mean} (average SUV of all ^{18}F-NaF–positive FD lesions); (iii) total volume of all ^{18}F-NaF–positive FD lesions (TV); and (iv) total FD lesion activity determined as the product of TV multiplied by SUV_{mean} ($TA = TV \times SUV_{mean}$) (TA). Skeletal outcomes, functional outcomes, and bone turnover markers were correlated with ^{18}F-NaF PET/CT parameters. TV and TA of extracranial FD lesions correlated strongly with skeletal outcomes including fractures and surgeries (p values ≤ 0.003). Subjects with impaired ambulation and scoliosis had significantly higher TV and TA values ($P < 0.05$), obtained from extracranial and spinal lesions, respectively. Craniofacial surgeries correlated with TV and TA of skull FD lesions ($P < 0.001$). Bone turnover markers, including alkaline phosphatase, N-telopeptides, and osteocalcin, were strongly correlated with TV and TA ($P < 0.05$) extracted from FD lesions in the entire skeleton. No associations were identified with SUV_{max} or SUV_{mean}. Bone pain and age did not correlate with ^{18}F-NaF PET/CT parameters. FD burden evaluated by ^{18}F-NaF-PET/CT facilitates accurate assessment of FD activity, and correlates quantitatively with clinically-relevant skeletal outcomes. © 2019 American Society for Bone and Mineral Research.

KEY WORDS: ANALYSIS/QUANTITATION OF BONE (OTHER); BIOCHEMICAL MARKERS OF BONE TURNOVER; DISEASES AND DISORDERS OF/RELATED TO BONE (OTHER)

Introduction

Fibrous dysplasia (FD) is an uncommon disorder characterized by replacement of normal bone and marrow with fibro-osseous tissue.[1] Somatic activating mutations in *GNAS* lead to discrete, expansile skeletal lesions prone to fracture and deformity, resulting in pain and physical impairment.[2,3] Patients present along a broad clinical spectrum with a phenotype that varies widely between individuals. FD may affect one bone (monostotic) or multiple (polyostotic) and may occur in isolation or in combination with extraskeletal manifestations, including skin macules and hyperfunctioning endocrinopathies. The combination of FD and one or more extraskeletal features is termed McCune-Albright syndrome (MAS).[1] Current clinical management in FD is inadequate. There are no medical therapies that have been shown to prevent FD lesion expansion or associated skeletal deformities.[4–6] Surgical treatment is the mainstay approach for fractures and deformities; however, outcomes are frequently unsatisfactory due to postoperative FD regrowth in the craniofacial skeleton,[7,8] and implants that are incapable of providing adequate long-term support in weight-bearing bones, particularly in growing children.[9–11]

Because of the wide phenotypic variability between patients, accurate assessment of skeletal disease burden is a critical component of the evaluation, management, and study of FD.[1] Radiographs and computed tomography (CT) scans can provide anatomical characterization of individual FD lesions

Received in original form November 2, 2018; revised form March 20, 2019; accepted March 27, 2019. Accepted manuscript online May 22, 2019.
Address correspondence to: Alison M Boyce, MD, National Institutes of Health, 30 Convent Drive Room 228 MCS 4320, Bethesda, MD 20892, USA. E-mail: boyceam@mail.nih.gov
Additional Supplementary information may be found in the online version of this article.

Journal of Bone and Mineral Research, Vol. 34, No. 9, September 2019, pp. 1619–1631
DOI: 10.1002/jbmr.3738

(Fig. 1*A*, *B*); however, nuclear medicine studies are necessary to determine total skeletal involvement.[12] The most commonly used method is the Skeletal Burden Score, a 99m-technetium-methylene diphosphonate (^{99m}Tc-MDP)-based technique that assesses the percentage of the skeleton involved with FD[13] (Fig. 1*C*, *D*). This is a reliable, reproducible technique that correlates with mobility impairment.[13] However, Skeletal Burden Score is based on visual interpretation of conventional bone scans and lacks the quantitative capability to evaluate and monitor activity within individual lesions. Because of this important limitation, Skeletal Burden Score is an inadequate surrogate endpoint for trials of bone-altering therapies.[4,14,15] Thus, there is a critical need to identify surrogate endpoints that are capable of accurately quantifying FD lesion activity, while correlating with clinically meaningful outcomes.

^{18}F-NaF is a bone-seeking positron emitting radiopharmaceutical which is taken up through ($^{18}F^-$) ions, which exchange with hydroxyl ions (OH^-) on the surface of hydroxyapatite-forming fluoroapatite.[16] Skeletal sites with increased ^{18}F-NaF activity reflect underlying bone processes, such as those in FD, which lead to increased bone crystal surface exposed to blood flow, resulting in higher availability of radiotracer binding sites.[17–19] The hybridization of PET imaging with multisection CT allows for simultaneous anatomic evaluation of skeletal lesions, which is an attractive capability in deforming bone disorders such as FD. This technique has been applied widely to evaluate skeletal tumor burden and activity in metastatic diseases.[20–23]

The purpose of this study was to investigate the clinical utility of ^{18}F-NaF PET/CT imaging in patients with FD. We hypothesized that FD burden determined by ^{18}F-NaF PET/CT imaging would correlate with FD-related skeletal outcomes and biochemical markers of FD activity.

Materials and Methods

Subjects

Subjects were evaluated as part of a long-standing NIH natural history study in FD/MAS (NCT00001727). This protocol involves collection of a standard set of data elements at the NIH Clinical Center, obtained through history and physical examination, physiatric, neuro-ophthalmologic and audiology evaluations, and biochemical testing. Subjects receive medical treatment for MAS-associated endocrinopathies and undergo imaging studies as clinically indicated. Nuclear medicine scans are clinically indicated to assess total skeletal disease burden at the time of diagnosis of FD/MAS, and at 3-year to 5-year intervals for patients experiencing skeletal complications. Fifteen consecutively enrolled subjects who met clinical indications for nuclear medicine scanning underwent whole-body ^{18}F-NaF PET/CT studies between 2012 and 2016. The protocol was approved by the NIDCR Institutional Review Board, and all subjects and/or their guardians gave informed consent/assent. The diagnosis of FD/MAS was established on clinical grounds with molecular testing as needed, according to previously published guidelines.[1]

^{18}F-NaF PET/CT studies

^{18}F-NaF PET/CT scans were obtained on dedicated PET/CT scanners, after intravenous injection of an average ± standard deviation (SD) of 2.81 ± 0.83 mCi of ^{18}F-sodium fluoride (range, 0.92 to 4.98 mCi). For adolescent and adult subjects, the injected dose ranged from 2.06 to 4.98 mCi; for one pediatric subject (age 6 years), a weight-based dose of 0.04 mCi/kg was administered. Scanners were Siemens Biograph 128_mCT models (Siemens Medical Solutions USA, Inc., Malvern, PA, USA), with FlowMotion positioning and 256 × 256 matrix size. PET images from the vertex of the skull to the plantar surface of the feet were acquired, 62.36 ± 6.11 (mean ± SD) min (range, 58 to 76 minutes) post-tracer injection. Standardized uptake values (SUVs) were measured on time-of-flight (TOF) PET images and were normalized to total body weight (as opposed to lean body mass or body surface area). A noncontrast, low-dose CT scan was performed for attenuation correction and co-registration. Representative images are shown in Fig. 2*A*-*D*.

Determination of FD burden

Whole-body skeletal FD burden was assessed by quantifying 18F-NaF activity using the MIM Vista workstation (version 6.5.9; MIM Software Inc., Cleveland, OH, USA) (Fig. 3*A*). A volume of interest (VOI) encompassing the entire skeleton was drawn (Fig. 3*B*), and subsequently a SUV threshold–based approach customized per subject was applied to include all disease-related bone uptake. The software enables automatic generation of separate VOIs encircling all areas above the SUV threshold set by the user (Fig. 3*C*). Automatic lesion demarcation generated by the software was compared with the lesions' anatomic cross-sectional images, to achieve maximal overlap with < 5% qualitative difference between functional and anatomic images. This approach was implemented to customize the applied SUV threshold per subject to the entire skeleton, avoiding incomplete segmentation of pathologic activity or inclusion of background physiologic uptake. Subsequently, an experienced nuclear medicine physician (GZP), blinded to subject clinical data, manually excluded areas with physiologic or non–FD-related ^{18}F-NaF activity (Fig. 3*D*). Non–FD-related ^{18}F-NaF activity was defined by uptake in the urinary tract (kidneys, ureters, urinary bladder, etc.) and any abnormal skeletal uptake that did not correspond to confirmed areas of FD involvement on corresponding CT imaging. Non–FD-related skeletal activity was identified and excluded in three subjects: (i) an area of focal increased uptake in a sacroiliac joint, consistent with sacroiliitis (Fig. 2*C*); (ii) an isolated area of focal increased uptake in a posterior mandible, subsequently found to be associated with a dental infection; and (iii) growth plate activity in a child. Finally, the following parameters were automatically obtained: (i) SUV of the FD lesion with the highest uptake (SUV_{max}); (ii) average SUV of all ^{18}F-NaF–positive FD lesions, determined as the mean of all ^{18}F-NaF-positive lesions' means (SUV_{mean}); (iii) whole-skeleton disease indices of total volume by summation of the volumes of all ^{18}F-NaF avid FD lesions (TV); and (iv) total lesion activity, determined as the product of SUV_{mean} multiplied by total volume of all ^{18}F-NaF avid FD lesions seen on PET/CT (TA = SUV_{mean} × TV) (TA). PET/CT parameters were separately assessed for FD lesions in the skull, spine, and extracranial skeleton to investigate correlations with clinical and functional outcomes related to these specific regions. The quantification analysis for all ^{18}F-NaF parameters was performed twice blindly by the same reader. By employing the same quantification approach, the obtained parameters (SUVmax, SUVmean, TV, TA) from each scan exhibited an intraobserver variation of < 2% [(Value obtained from the 2nd analysis − Value obtained from the 1st analysis)/(Value obtained from the 1st analysis) × 100].

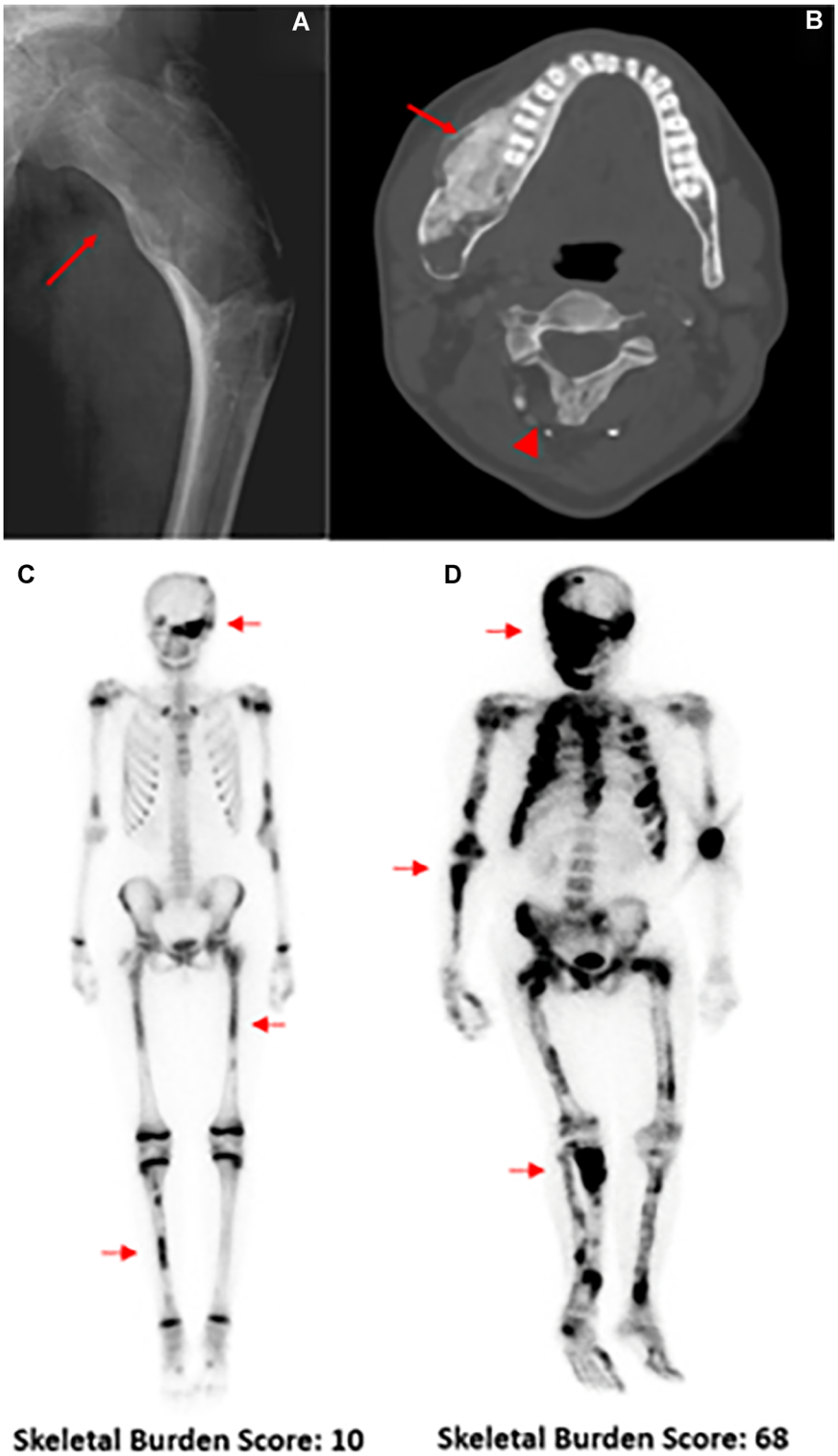

Fig. 1. Representative images demonstrating typical radiographic features in fibrous dysplasia. (*A*) X-ray of the proximal femur shows a discrete, expansile lesion with a homogeneous, "ground glass" appearance. Note the characteristic cortical thinning, and coxa vara deformity of the femoral neck shaft (red arrow). (*B*) Axial computed tomography of the skull shows an expansile lesion with a homogenous, "ground glass" appearance in the mandible (red arrow). A smaller expansile lesion is also seen in the spinous process (red arrowhead). (*C*, *D*) Whole-body ^{99m}Tc-MDP bone scans from two individuals demonstrate patchy tracer uptake consistent with mosaic disease (red arrowheads); (*C*) shows mild disease affecting only a few regions with a Skeletal Burden Score of 10, and (*D*) shows severe disease affecting most of the skeleton with a Skeletal Burden Score of 68. The bone scan shown in *C* was obtained from a child with FD, as indicated by the increased tracer uptake at the growth plates.

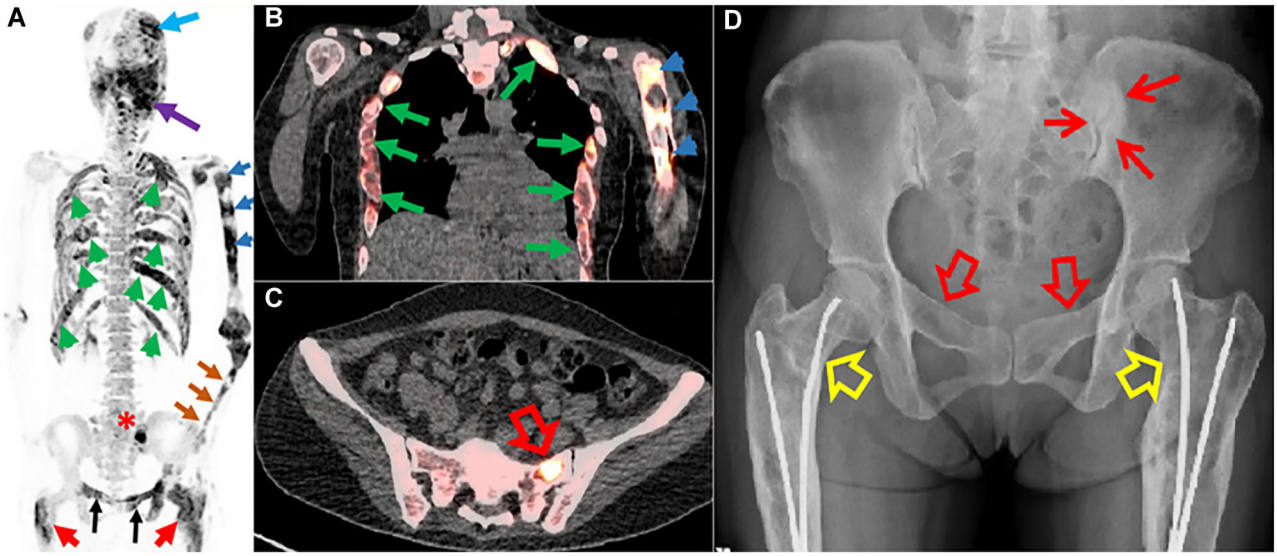

Fig. 2. Representative ^{18}F-NaF PET/CT images demonstrating features of fibrous dysplasia. (*A*) ^{18}F-NaF MIP PET image of the skull and torso showing multiple areas of abnormally increased uptake corresponding to FD lesions involving the skull (light blue arrow), facial bones (purple arrow), left humerus (short deep blue arrows), multiple ribs (short green arrows), left radius (orange arrows), both pubic rami (black arrows), and both femurs (red arrows). Uptake in the left sacroiliac joint (red star) corresponds to site of FD-unrelated osteosclerosis seen on CT (*C*, open red arrows) and X-ray (*D*, closed red arrows). (*B*) Coronal ^{18}F-NaF PET/CT image of the chest showing ^{18}F-NaF avid FD lesions in several ribs (green arrows) and throughout the left humerus (short deep blue arrows). (*C*) Axial ^{18}F-NaF PET/CT image of the pelvis showing focally increased uptake at the site of osteosclerosis in the left sacroiliac joint (open red arrow). (*D*) Anterior-posterior X-ray of the pelvis showing subarticular sclerosis on both sides of the ipsilateral left sacroiliac joint (closed red arrows), suggestive of likely sacroiliitis. FD lesions are apparent in both pubic rami (open red arrows) and proximal femoral bones with intramedullary rods noted on both femurs (open yellow arrows). MIP = maximum intensity projection.

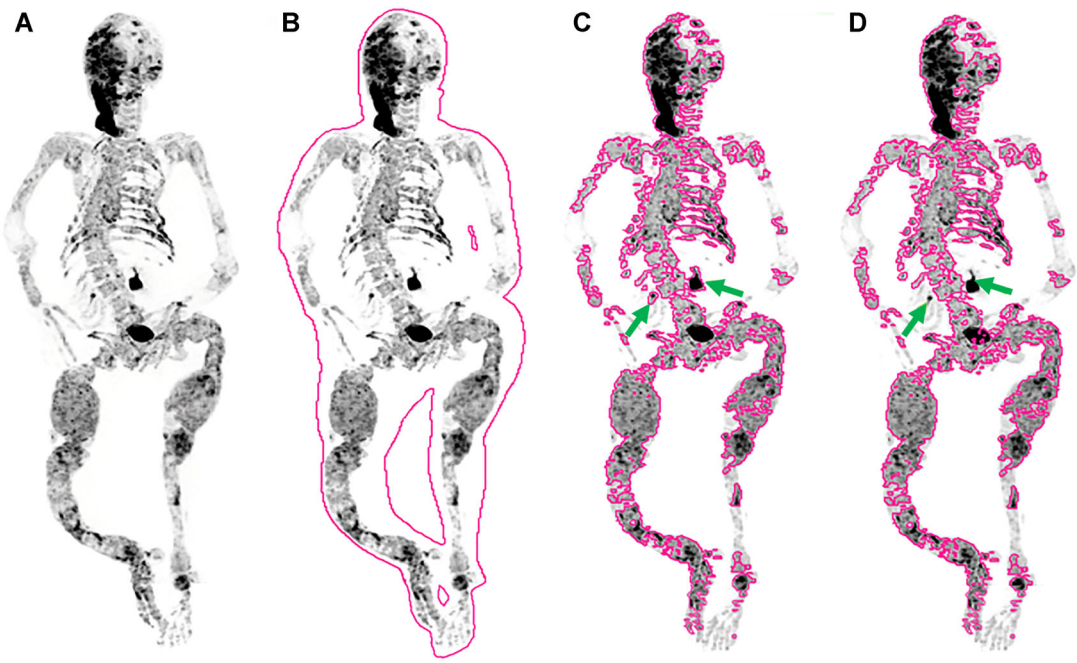

Fig. 3. Representative images showing semiautomated approach for quantification of FD-related ^{18}F-NaF activity. (*A*) Whole-body ^{18}F-NaF PET image of a patient with FD, showing abnormal radiotracer distribution. (*B*) Semiautomated drawn VOI encompassing the entire skeleton. (*C*) Automatically generated VOI post SUV-threshold application, encircling all areas with uptake above the threshold. (*D*) Final VOI after manual extraction of areas with physiologic (eg, kidneys, urinary bladder) and FD-unrelated activity (for example, the osteosclerotic lesion demonstrated in Fig. 2). Green arrows in *C* and *D* show ^{18}F-NaF activity in the kidneys, which was excluded from the final VOI. MIP = maximum intensity projection; VOI = volume of interest.

Clinical outcome measures

The following skeletal-related clinical outcome measures were evaluated: (i) fractures, (ii) orthopedic surgeries, (iii) impaired ambulation, (iv) scoliosis, (v) craniofacial surgeries, (vi) optic neuropathy, (vii) hearing loss, and (viii) bone pain. Outcome measures were determined by retrospective review of clinical data elements collected on the natural history study. Fracture, surgery, and pain data were obtained by review of history and physical examinations. Ambulation impairment was defined as regular use of one or more assistive ambulation devices and was obtained by physiatric evaluation. Spinal radiographs were performed in patients with known spinal FD involvement and/or evidence of spinal curvature on examination, and scoliosis was defined as a Cobb angle of > 10 degrees on radiographs.[5] Optic neuropathy was determined by neuro-ophthalmologic evaluation, and hearing loss was determined by audiologic evaluation. These clinical outcome measures were correlated with ^{18}F-NaF-PET/CT parameters (SUV_{max}, SUV_{mean}, TV, and TA). ^{18}F-NaF-PET/CT parameters were also correlated with subject age and biochemical bone turnover markers alkaline phosphatase, osteocalcin, and N-telopeptides (NTX).

Statistical analysis

Statistical analyses were performed using R software (version 3.3; R Foundation for Statistical Computing, Vienna, Austria; https://www.r-project.org/). Descriptive statistics were used to characterize subjects, and data were expressed as mean ± SD. Correlations between FD-related ^{18}F-NaF PET/CT parameters and continuous clinical outcome measures were quantified using Pearson's (*r*) or Spearman's (rho) correlation coefficient calculations with bootstrap 95% confidence intervals (CIs) calculated from 100 iterations where appropriate. The strength of each correlation was distinguished as "very weak," "weak," "moderate," "strong," and "very strong" for an absolute correlation coefficient lying in range of [0.0 – 0.19], [0.2 – 0.39], [0.4 – 0.59], [0.6 – 0.79] and [0.8 – 1], respectively.[24] Scatterplots with a linear regression and 95% CIs were generated to assess the relationship between age, clinical outcome measures, and bone turnover markers with ^{18}F-NaF PET/CT parameters. Statistical diagnostic tests regarding linearity, homoscedasticity, normality of residuals and outliers were performed for validation of the regression analysis results. Mann-Whitney-Wilcoxon test was used to assess potential differences based on categorical FD variables (impaired ambulation, scoliosis, optic neuropathy, hearing loss, pain), in association with ^{18}F-NaF PET/CT parameters, with box-plots depicting the different subject groups. For all tests, a *p* value of less than 0.05 was considered to indicate statistical significance. Values of *p* were adjusted to account for multiple hypothesis testing using Benjamini and Hochberg false discovery rate correction.

Results

Study population

Subject characteristics are included in Table 1. The study population was clinically heterogeneous, representing a wide range of ages, clinical outcome measures, and FD involvement. The subjects' racial identities included non-Hispanic white (12/15; 80%), black or African American (2/15; 13%), and Asian (1/15; 7%). All subjects had polyostotic FD, defined as the presence of two or more noncontiguous FD lesions. The mean age and SD were 27 ± 12 years (range, 6 to 57 years), and included 10 female subjects and five male subjects. No subjects had clinical evidence of fractures or active malignancies at the time of scanning. One 28-year-old female subject had a history of FD-associated osteosarcoma of the left mandible diagnosed at age 12 years, for which she underwent hemimandibulectomy. She did not require further treatment for her malignancy and has had no signs of recurrence or metastases.

Correlation between ^{18}F-NaF PET/CT parameters and skeletal outcomes

Extracranial clinical outcomes

Correlations were evaluated between clinical outcomes involving the extracranial skeleton (ie, entire skeleton excluding the skull) and ^{18}F-NaF PET/CT parameters for extracranial FD (Table 2, Fig. 4). TV and TA of extracranial FD showed very strong correlation with lifetime fractures and mean fractures per year (Fig. 4*A–D*). Strong correlations were also observed between TV and TA of extracranial FD and lifetime orthopedic surgeries and mean orthopedic surgeries per year (Fig. 4*E–H*). Extracranial SUV_{max} or SUV_{mean} did not correlate with the prevalence of fractures or surgeries.

Subjects with impaired ambulation had significantly higher TV and TA of extracranial FD in comparison to patients with full mobility (Table 3). No associations were identified with extracranial SUV_{max} or SUV_{mean}.

^{18}F-NaF PET/CT parameters were separately assessed for spinal FD lesions and correlated with the presence of spinal deformity (Fig. 5*A* and *B*, Table 3). Spinal TV and TA were significantly higher in subjects with scoliosis versus subjects without scoliosis. No associations were identified with spinal SUV_{max} or SUV_{mean}.

Craniofacial outcomes

Correlations were evaluated between craniofacial outcomes and ^{18}F-NaF PET/CT parameters for FD affecting the skull (Table 2, Fig. 6). Craniofacial TV and TA were strongly associated with lifetime craniofacial surgeries (Fig. 6*A*, *B*) and mean craniofacial surgeries per year (Fig. 6*C*, *D*). Craniofacial SUV_{max} or SUV_{mean} did not correlate with the prevalence of craniofacial surgeries. There were no associations between craniofacial ^{18}F-NaF PET/CT parameters and the presence of optic neuropathy or hearing loss.

Pain

There were no significant differences in ^{18}F-NaF PET/CT parameters in the entire skeleton between subjects with and without bone pain (Table 3).

Correlation between ^{18}F-NaF PET/CT parameters and bone turnover markers

TV and TA of FD in the entire skeleton strongly correlated with serum levels of alkaline phosphatase, osteocalcin, and NTX) (Table 4, Fig. 7*A-F*). Neither skeletal SUV_{max} nor SUV_{mean} showed significant correlation with bone turnover markers (Table 4).

Table 1. Subject Characteristics

Age (years) and sex	Race	MAS endocrine features	FD location	Lifetime fractures/ mean rate per year[a]	Lifetime orthopedic surgeries/ mean rate per year[a]	Lifetime craniofacial surgeries/ mean rate per year[a]	Other clinical outcome measures
6F	W	GH	Cf	0	0	0	None
17F	W	PP, GH	Cf, Ax	1/0.06	0	1/0.06	Hearing loss, pain
18F	W	None	Cf	0	0	0	Optic neuropathy
22F	W	PP	Cf, Ax, Ap	2/0.1	0	0	Pain
22F	W	PP, HT, PW	Cf, Ax, Ap	100/4.6	52/2.4	3/0.1	Impaired ambulation, scoliosis, pain
23M	W	PW	Cf, Ax, Ap	4/0.2	0	0	Scoliosis, pain
24M	W	None	Cf, Ap	0	0	0	Pain
25M	W	GH	Cf, Ax, Ap	10/0.4	0	1/0.04	Scoliosis, pain
27F	B	PP	Cf, Ax, Ap	20/0.8	6/0.2	6/0.2	Scoliosis, pain
28F	A	PP, HT, GH, PW	Cf, Ax, Ap	6/0.2	9/0.3	6/0.2	Hearing loss, pain
30M	W	PW	Cf, Ax, Ap	36/1.2	6/0.2	2/0.07	Impaired ambulation, scoliosis, pain
31F	B	GH	Cf, Ap	0	0	1/0.03	Optic neuropathy
39F	W	None	Ap	1/0.03	2/0.05	0	Pain
47F	W	PP, HT, PW	Cf, Ax, Ap	50/1.1	7/0.2	0	Impaired ambulation, scoliosis, optic neuropathy, pain
57M	W	PP, PW	Cf, Ax, Ap	40/0.7	34/0.6	0	Impaired ambulation, scoliosis, pain

MAS = McCune-Albright syndrome; FD = fibrous dysplasia; F = female; W = non-Hispanic white; GH = growth hormone excess; Cf = craniofacial skeleton; PP = precocious puberty; Ax = axillary skeleton; Ap = appendicular skeleton; HT = hyperthyroidism; PW = phosphate wasting; M = male; B = black or African American; A = Asian.

[a]Mean rate per year determined by number of total lifetime events divided by years of life.

Table 2. Correlation Between Continuous Clinical Outcome Measures and ^{18}F-NaF PET/CT Parameters

Parameter	Lifetime fractures[a]	Mean fractures per year[a]	Lifetime orthopedic surgeries[a]	Mean orthopedic surgeries per year[a]	Lifetime craniofacial surgeries[b]	Mean craniofacial surgeries per year[b]
SUV_{max}	rho = 0.513, P = 0.113	rho = 0.458, P = 0.184	rho = 0.303, P = 0.442	rho = 0.254, P = 0.546	rho = 0.008, P = 1.000	rho = –0.004, P = 1.000
SUV_{mean}	rho = 0.114, P = 0.824	rho = 0.083, P = 0.904	rho = 0.175, P = 0.694	rho = 0.171, P = 0.694	rho = 0.028, P = 0.998	rho = 0.019, P = 0.998
TV	rho = 0.897, P < 0.001	rho = 0.873, P < 0.001	rho = 0.825, P = 0.001	rho = 0.805, P = 0.002	rho = 0.831, P < 0.001	rho = 0.835, P < 0.001
TA	rho = 0.870, P < 0.001	rho = 0.844, P < 0.001	rho = 0.801, P = 0.002	rho = 0.775, P = 0.003	rho = 0.855, P < 0.001	rho = 0.860, P < 0.001

Values are Spearman's rank correlation coefficients and corresponding p values adjusted for false discovery rate.

SUV_{max} = standardized uptake value of the FD lesion with the highest uptake; FD = fibrous dysplasia; SUV_{mean} = average standardized uptake value of all ^{18}F-NaF–positive FD lesions; TV = volumes of all ^{18}F-NaF avid FD lesions; TA = total lesional activity.

[a]Analyses performed for the extracranial skeleton.

[b]Analyses performed for the cranial skeleton.

Correlation between ^{18}F-NaF PET/CT parameters and age

There were no significant associations between 18F-NaF PET/CT parameters and subject age at the time of scanning (Table 4).

Comparison between ^{18}F-NaF PET/CT and ^{99m}Tc-MDP scintigraphy for FD lesion detection

Analyses were performed to compare the ability of ^{18}F-NaF PET/CT and ^{99m}Tc-MDP scintigraphy (considered the present standard of care for FD lesion identification) to detect total skeletal FD involvement. Analyses were limited to adult subjects ≥age 18 years, after which total skeletal disease burden is expected to remain stable.[25] Skeletal Burden Scores were determined for seven subjects who had previously undergone ^{99m}Tc-MDP scans and compared to Skeletal Burden Scores determined from ^{18}F-NaF PET/CT scans, using previously described methodology.[13] The median ^{99m}Tc-MDP-derived Skeletal Burden Score was 52.5 (interquartile range, 44.8, 67.9; range, 10.9 to 75), and the median ^{18}F-NaF-derived Skeletal Burden Score was 59.5 (interquartile range, 41.2, 71.8; range, 9.95 to 75). The median difference between the scans was 0 (interquartile range, –2.9, 3.9; range, –3.6 to 7.0). Linear regression analyses showed very strong correlation between Skeletal Burden Scores derived from both scan types ($R^2 = 0.98$, $P < 0.0001$) (Supporting Fig. 1).

Discussion

Accurate detection and quantification of skeletal lesions is important to determine prognosis, guide management, and serve as endpoints for clinical studies in patients with FD. This is the first study to show that FD-related ^{18}F-NaF uptake correlates with skeletal outcomes in this disorder. Strong and consistent correlations were observed between TV and TA of all skeletal ^{18}F-NaF avid FD lesions with bone turnover markers, suggesting this imaging technique is capable of accurately reflecting underlying bone metabolism in FD. Clinically-relevant outcomes such as fractures and surgeries were very strongly associated with volume and activity of lesions assessed by ^{18}F-NaF PET/CT. Finally, ^{18}F-NaF parameters TV and TA extracted from ^{18}F-NaF–positive FD lesions in the extracranial skeleton, craniofacial skeleton, spine, and entire skeleton were able to differentiate patients with critical disease-related features involving these areas, including impaired ambulation, scoliosis, and pain.

SUV-based measures normalized to patient body weight, lean body mass, or body surface area are the most commonly used semiquantitative tools in PET-imaging.[26] However, in our study the obtained SUVmetrics (SUV_{mean} and SUV_{max}) did not show any correlation with clinical or biochemical measures of disease. FD is a benign disorder in which complications arise due to structural instability of abnormal bone; it is therefore intuitive that prognosis is determined in large part by the overall volume of affected tissue, which is not directly accounted for using SUV-based metrics. This is consistent with a growing body of evidence that radiotracer-avid lesion volume and lesion activity may also outperform SUV-based measurements in other polyostotic conditions, such as metastatic bone disease.[21,27–29]

The optimal SUV threshold values for application of ^{18}F-NaF PET/CT have not been standardized and should be determined based on the underlying pathologic condition and the goals of

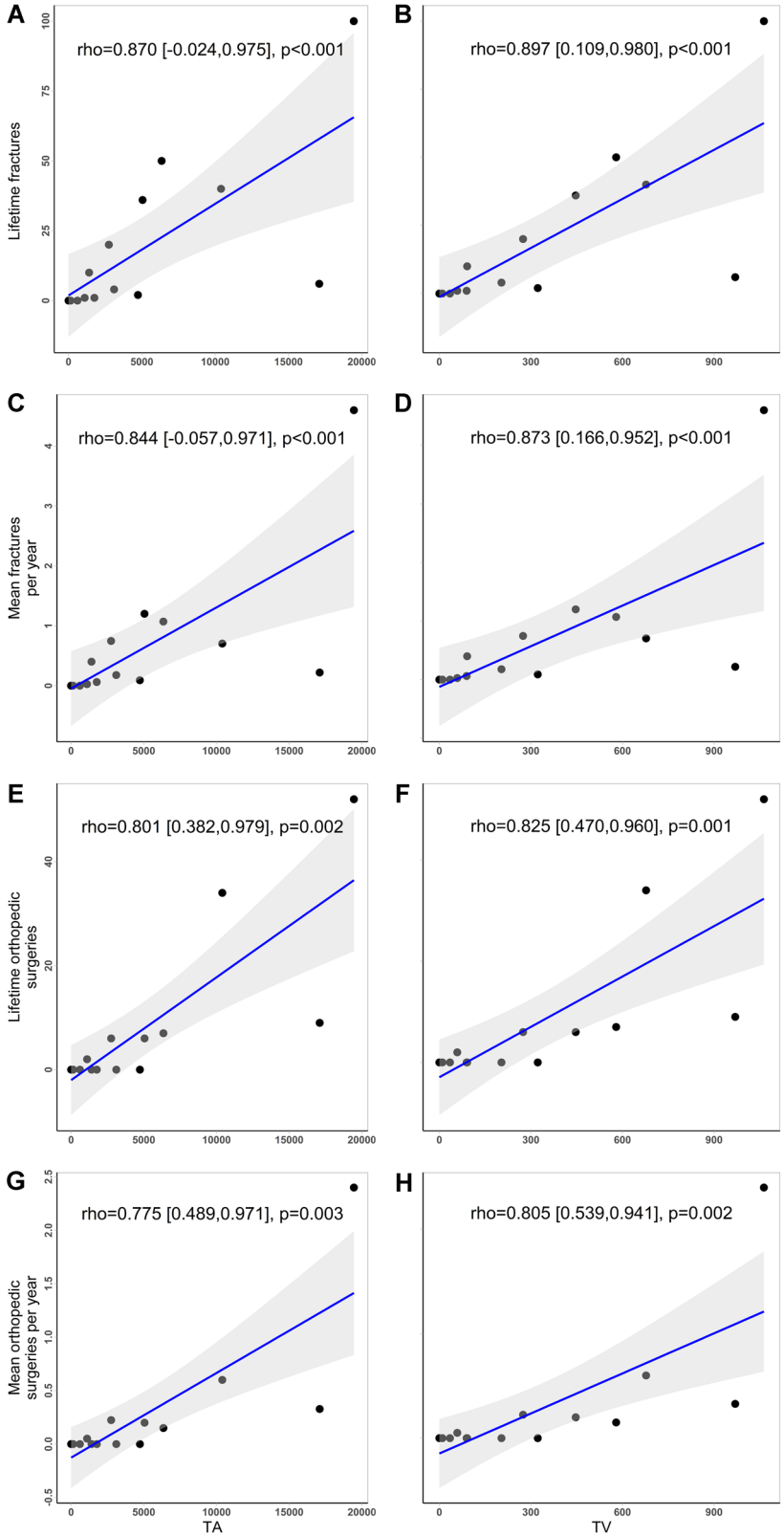

Fig. 4. Correlation between ^{18}F-NaF PET/CT parameters and extracranial skeletal outcomes. Scatter plot and linear regression with 95% confidence intervals depicting TA and TV values, respectively, for FD-related activity in the extracranial skeleton in relation to lifetime fractures (*A*, *B*), mean fractures per year (*C*, *D*), lifetime orthopedic surgeries (*E*, *F*), and mean orthopedic surgeries per year (*G*, *H*).

Table 3. Correlation Between Categorical Clinical Outcome Variables and ^{18}F-NaF PET/CT Parameters

Parameter	Impaired ambulation[a]	Scoliosis[b]	Pain[c]	Optic neuropathy[d]	Hearing loss[d]
SUV_{max}	$P = 0.357$	$P = 0.558$	$P = 0.694$	$P = 0.202$	$P = 0.649$
SUV_{mean}	$P = 0.998$	$P = 1.000$	$P = 0.112$	$P = 0.242$	$P = 0.270$
TV	$P = 0.043$	$P = 0.012$	$P = 0.077$	$P = 0.933$	$P = 0.649$
TA	$P = 0.043$	$P = 0.014$	$P = 0.077$	$P = 0.933$	$P = 0.221$

Values are Spearman's rank correlation coefficients and corresponding *p* values adjusted for false discovery rate.

SUV_{max} = standardized uptake value of the FD lesion with the highest uptake; FD = fibrous dysplasia; SUV_{mean} = average standardized uptake value of all ^{18}F-NaF–positive FD lesions; TV = volumes of all ^{18}F-NaF avid FD lesions; TA = total lesional activity.

[a]Analyses performed for the extracranial skeleton.

[b]Analyses performed for the spine.

[c]Analyses performed for the total skeleton.

[d]Analyses performed for the craniofacial skeleton.

the evaluation. In several oncologic studies of patients with prostate cancer, researchers used an SUV threshold > 15 for ^{18}F-NaF uptake to segment bone metastases.[22,30] In other oncologic studies utilizing ^{18}F-NaF PET/CT scans to evaluate metastatic diseases from a variety of cancer types, an SUV threshold of > 10 was applied.[20,21] In the current study, SUV thresholds ranged between 7 and 8. The lower thresholds in this study likely reflect the benign nature of FD, where normal bone and marrow are replaced by fibro-osseous rather than malignant tissue.

^{18}F-NaF PET/CT offers considerable advantages over current clinical assessment tools in FD. Clinical trials have been severely limited by a lack of surrogate markers capable of reflecting FD activity. To date, Skeletal Burden Score using ^{99m}Tc-MDP scintigraphy has been the only imaging technique capable of assessing disease burden and associating with ambulation outcomes.[13] A direct comparison between ^{18}F-NaF and ^{99m}Tc-MDP scans in this study showed that both methodologies appear to be equally effective in determining Skeletal Burden Score. Because Skeletal Burden Score measures only the extent of affected tissue, it has been shown to remain static throughout adulthood after FD lesions have been fully established.[25] It is therefore not a useful endpoint for evaluating response to bone-altering therapies, which may potentially decrease lesion activity and improve bone quality but are unlikely to affect the size of established lesions. Bone turnover markers are typically elevated in patients with FD and may also serve as potential quantitative endpoints.[4] However, FD-specific serum markers have not been identified, and it is therefore unfeasible to use bone turnover markers to quantify response to bone-altering therapies that affect both FD and non-FD bone. The unique quantitative capabilities offered by ^{18}F-NaF PET/CT imaging, together with the vastly superior resolution of PET-imaging compared to conventional gamma camera imaging, represent a considerable advantage and may potentially have the capacity to serve as a clinically relevant, quantitative surrogate endpoint for clinical trials in FD.

The detailed morphological characterization provided by the multisection CT component of ^{18}F-NaF PET/CT imaging offers another important advantage. Unlike ^{18}F-NaF PET/CT, traditional ^{99m}Tc-MDP scans are unable to provide sufficient anatomical information for a thorough clinical assessment of FD lesions, and must be accompanied by additional imaging studies such as radiographs or CT scans. The combination of disease quantification and anatomical imaging may be particularly advantageous in evaluating craniofacial and spinal FD, where TA and TV of these skeletal compartments correlated with region-specific complications (ie, craniofacial surgeries and scoliosis). The presence of skeletal deformities does not confound the ability of ^{18}F-NaF to demarcate FD lesions, because this process is fully automated upon application of the SUV threshold. In addition, the favorable ^{18}F-NaF

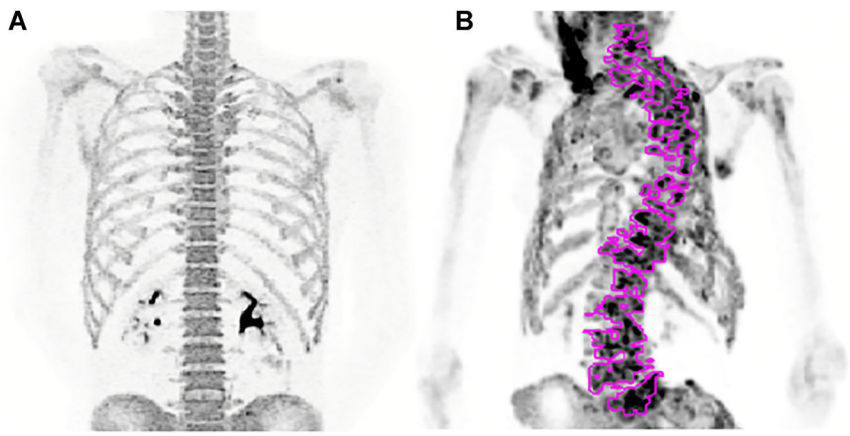

Fig. 5. ^{18}F-NaF PET spinal imaging. (*A*) ^{18}F-NaF PET image of the torso showing normal radiotracer distribution in a spine unaffected by FD. (*B*) ^{18}F-NaF PET image of the torso showing spinal deformity with diffusely increased activity and the semiautomated generated VOI encompassing all spinal FD-related ^{18}F-NaF activity.

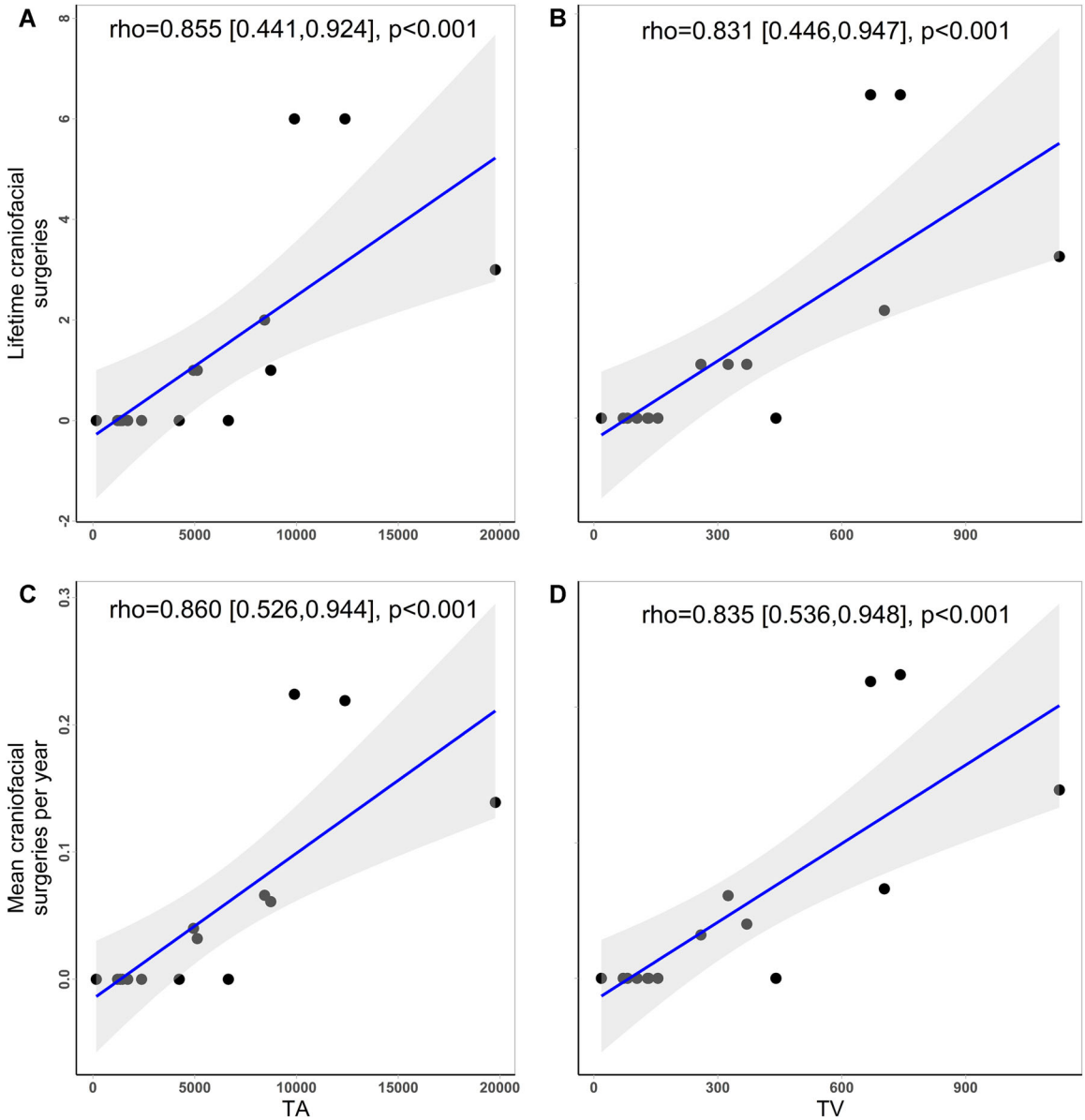

Fig. 6. Correlation between ^{18}F-NaF PET/CT parameters and craniofacial outcomes. Scatter plot and linear regression with 95% confidence intervals depicting TA and TV values, respectively, for FD-related activity in the craniofacial skeleton in relation to lifetime craniofacial surgeries (*A*, *B*) and mean craniofacial surgeries per year (*C*, *D*).

Table 4. Correlation Between ^{18}F-NaF PET/CT Parameters, Bone Turnover Markers, and Age

Parameter	Alkaline phosphatase (U/L)	Osteocalcin (ng/mL)	N-telopeptides (nmol/mmol)	Age (years)
SUV_{max}	$r = -0.252$, $P = 0.546$	$r = -0.355$, $P = 0.333$	$r = -0.287$, $P = 0.540$	$r = 0.141$, $P = 0.769$
SUV_{mean}	$r = -0.135$, $P = 0.774$	$r = -0.445$, $P = 0.200$	$r = -0.072$, $P = 0.933$	$r = -0.519$, $P = 0.112$
TV	$r = 0.685$, $P = 0.015$	$r = 0.760$, $P = 0.005$	$r = 0.670$, $P = 0.037$	$r = 0.380$, $P = 0.287$
TA	$r = 0.758$, $P = 0.005$	$r = 0.707$, $P = 0.012$	$r = 0.739$, $P = 0.014$	$r = 0.229$, $P = 0.587$

Values are Pearson's coefficients of correlation and corresponding *p* values adjusted for false discovery rate.

SUV_{max} = standardized uptake value of the FD lesion with the highest uptake; FD = fibrous dysplasia; SUV_{mean} = average standardized uptake value of all ^{18}F-NaF–positive FD lesions; TV = volumes of all ^{18}F-NaF avid FD lesions; TA = total lesional activity.

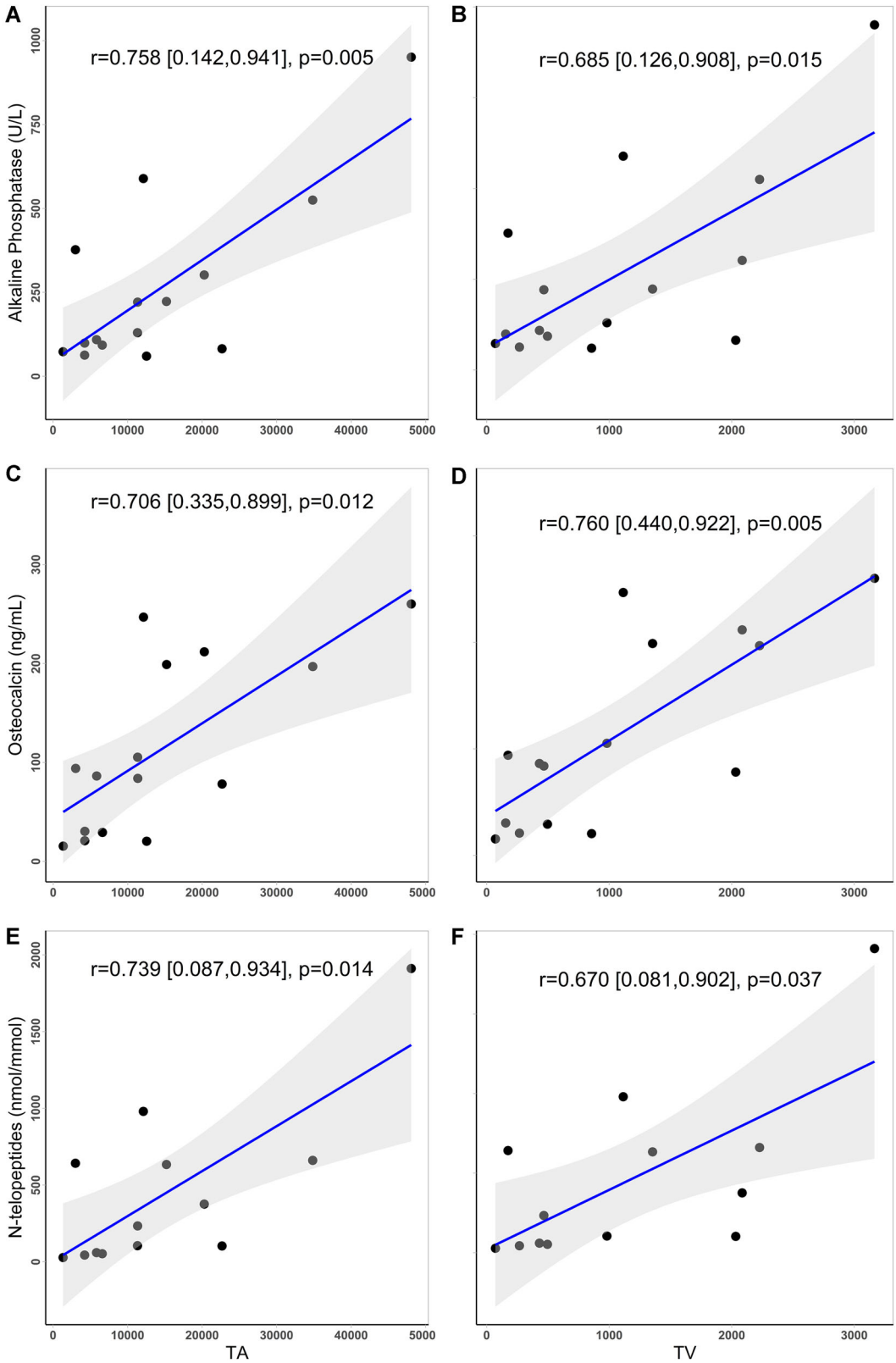

Fig. 7. Correlation between ^{18}F-NaF PET/CT parameters and bone turnover markers. Scatter plot and linear regression with 95% confidence intervals depicting TV and TA values for FD-related activity in the entire skeleton in relation to bone turnover markers, including alkaline phosphatase (*A*, *B*), urine-NTX (*C*, *D*), and osteocalcin (*E*, *F*)

pharmacokinetic characteristics compared to ^{99m}Tc- MDP, including minimal plasma protein binding and rapid soft-tissue clearance, result in shorter imaging times (< 1 hour after intravenous injection) and increased bone-to-background, leading to twice as great bone uptake and enhanced diagnostic accuracy compared to ^{99m}Tc- MDP scintigraphy.[17] This combination of quantitative capabilities, superior anatomical characterization, and improved diagnostic accuracy suggests that ^{18}F-NaF PET/CT imaging is the modality of choice for evaluation and monitoring of FD activity.

The primary limitations of this study are the relatively small subject numbers and the clinical heterogeneity between subjects. This is an inherent obstacle to rare disease research, where studies are frequently underpowered to detect statistically significant effects. However, in this study, strong correlations were observed despite the small number of subjects, and the clinical heterogeneity demonstrated the utility of this technique across a spectrum of disease. Additional studies with larger numbers of subjects are needed to verify the reproducibility of these findings, including interreader reproducibility analyses. Another important limitation was the cross-sectional design. Prospective studies with serial scans are needed to determine whether ^{18}F-NaF PET/CT scans can detect longitudinal changes in lesion activity over time in individual patients. Prospective studies are also needed to determine whether ^{18}F-NaF PET/CT scans are predictive of skeletal complications. In this study bone pain was evaluated categorically, and additional studies using validated quantitative pain measures are needed to determine the relationship between ^{18}F-NaF PET/CT parameters and pain. It is unknown if ^{18}F-NaF PET/CT uptake related to FD lesions can reliably be distinguished from uptake related to fractures and secondary malignancies, both of which are known complications in this disorder. In this study no subjects had clinical evidence of fractures or active malignancies at the time of scanning. However, if patients have concerning symptoms, such as acute-onset focal pain or rapid expansion of an FD lesion, clinical evaluation for fractures and/or malignancies should be performed before nuclear medicine scanning. Application of these findings therefore should involve collaboration between metabolic bone specialists and nuclear medicine specialists experienced in interpreting radionuclide scans.

^{18}F-NaF PET/CT imaging parameters demonstrate strong correlations with clinically relevant skeletal outcomes in patients with FD. These findings establish ^{18}F-NaF PET/CT as the current imaging modality of choice for evaluation of FD activity. In addition to its immediate clinical application, this technique holds potential as a surrogate endpoint for clinical trials, a critical area of need to improve outcomes for patients with FD.

Disclosures

The authors report no relevant disclosures.

Acknowledgments

This study was funded by the Intramural Research Program of the National Institute of Dental and Craniofacial Research, National Institutes of Health.

Authors' roles: Study design: GZP, MTC, and AMB. Study conduct: GZP, MTC, and AMB. Data collection: GZP and AMB. Data analysis: GZP, GCM, and AMB. Data interpretation: GZP, GCM, PF, AHK, UB, KM, and AMB. Drafting manuscript: GZP, GCM, and AMB. Revising manuscript content: GZP, GCM, and AMB. Approving final version of manuscript: GZP, GCM, PF, AHK, UB, KM, MTC, and AMB. AMB takes responsibility for the integrity of the data analysis.

References

1. Boyce AM, Florenzano P, de Castro LF, et al. Fibrous dysplasia/McCune-Albright syndrome. 2015 Feb 26 [updated 2018 Aug 16; cited 2019 Apr 16]. In: Adam MP, Ardinger HH, & Pagon RA, editors, *GeneReviews® [Internet]* (1993-2019). Seattle (WA). University of Washington, Seattle. Available from. https://www.ncbi.nlm.nih.gov/books/NBK274564/
2. Weinstein LS, Shenker A, Gejman PV, Merino MJ, Friedman E, Spiegel AM. Activating mutations of the stimulatory G protein in the McCune-Albright syndrome. N Engl J Med. 1991;325(24):1688–95.
3. Robinson C, Collins MT, Boyce AM. Fibrous dysplasia/McCune-Albright syndrome: clinical and translational perspectives. Curr Osteoporos Rep. 2016;14(5):178–86.
4. Boyce AM, Kelly MH, Brillante BA, et al. A randomized, double blind, placebo-controlled trial of alendronate treatment for fibrous dysplasia of bone. J Clin Endocrinol Metab. 2014;99(11):4133–40.
5. Berglund JA, Tella SH, Tuthill KF, et al. Scoliosis in fibrous dysplasia/McCune-Albright syndrome: factors associated with curve progression and effects of bisphosphonates. J Bone Miner Res. 2018;33(9):1641–8.
6. Florenzano P, Pan KS, Brown SM, et al. Age-related changes and effects of bisphosphonates on bone turnover and disease progression in fibrous dysplasia of bone. J Bone Miner Res. Forthcoming. Epub. 2019. Jan 15. https://doi.org/10.1002/jbmr.3649
7. Boyce AM, Burke A, Cutler Peck C, DuFresne CR, Lee JS, Collins MT. Surgical management of polyostotic craniofacial fibrous dysplasia: long-term outcomes and predictors for postoperative regrowth. Plast Reconstr Surg. 2016;137(6):1833–9.
8. Lee JS, FitzGibbon EJ, Chen Y, et al. Clinical guidelines for the management of craniofacial fibrous dysplasia. Orphanet J Rare Dis. 2012;7(Suppl 1):S2.
9. Stanton RP, Ippolito E, Springfield D, Lindaman L, Wientroub S, Leet A. The surgical management of fibrous dysplasia of bone. Orphanet J Rare Dis. 2012;7(Suppl 1):S1.
10. Leet AI, Boyce AM, Ibrahim KA, Wientroub S, Kushner H, Collins MT. Bone-grafting in polyostotic fibrous dysplasia. J Bone Joint Surg Am. 2016;98(3):211–9.
11. Majoor BCJ, Leithner A, van de Sande MAJ, Appelman-Dijkstra NM, Hamdy NAT, Dijkstra PDS. Individualized approach to the surgical management of fibrous dysplasia of the proximal femur. Orphanet J Rare Dis. 2018;13(1):72.
12. Kushchayeva YS, Kushchayev SV, Glushko TY, et al. Fibrous dysplasia for radiologists: beyond ground glass bone matrix. Insights Imaging. 2018;9(6):1035–56.
13. Collins MT, Kushner H, Reynolds JC, et al. An instrument to measure skeletal burden and predict functional outcome in fibrous dysplasia of bone. J Bone Miner Res. 2005;20(2):219–26.
14. Boyce AM, Chong WH, Yao J, et al. Denosumab treatment for fibrous dysplasia. J Bone Miner Res. 2012;27(7):1462–70.
15. Ganda K, Seibel MJ. Rapid biochemical response to denosumab in fibrous dysplasia of bone: report of two cases. Osteoporos Int. 2014;25(2):777–82.
16. Czernin J, Satyamurthy N, Schiepers C. Molecular mechanisms of bone 18F-NaF deposition. J Nucl Med. 2010;51(12):1826–9.
17. Bastawrous S, Bhargava P, Behnia F, Djang DS, Haseley DR. Newer PET application with an old tracer: role of 18F-NaF skeletal PET/CT in oncologic practice. Radiographics. 2014;34(5):1295–316.
18. Papadakis GZ, Millo C, Bagci U, Blau J, Collins MT. 18F-NaF and 18F-FDG PET/CT in Gorham-Stout disease. Clin Nucl Med. 2016;41(11):884–5.

19. Lee H, Lee KS, Lee WW. 18F-NaF PET/CT findings in fibrous dysplasia. Clin Nucl Med. 2015;40(11):912–4.
20. Rohren EM, Etchebehere EC, Araujo JC, et al. Determination of skeletal tumor burden on 18F-Fluoride PET/CT. J Nucl Med. 2015;56(10):1507–12.
21. Etchebehere EC, Araujo JC, Fox PS, Swanston NM, Macapinlac HA, Rohren EM. Prognostic factors in patients treated with 223Ra: the role of skeletal tumor burden on baseline 18F-Fluoride PET/CT in predicting overall survival. J Nucl Med. 2015;56(8):1177–84.
22. Lindgren Belal S, Sadik M, Kaboteh R, et al. 3D skeletal uptake of (18)F sodium fluoride in PET/CT images is associated with overall survival in patients with prostate cancer. EJNMMI Res. 2017;7(1):15.
23. Harmon SA, Perk T, Lin C, et al. Quantitative assessment of early [(18)F]sodium fluoride positron emission tomography/computed tomography response to treatment in men with metastatic prostate cancer to bone. J Clin Oncol. 2017;35(24):2829–37.
24. Evans JD. *Straightforward statistics for the behavioral sciences*. Pacific Grove, CA. Brooks/Cole Publishing, 1996
25. Hart ES, Kelly MH, Brillante B, et al. Onset, progression, and plateau of skeletal lesions in fibrous dysplasia and the relationship to functional outcome. J Bone Miner Res. 2007;22(9):1468–74.
26. Adams MC, Turkington TG, Wilson JM, Wong TZ. A systematic review of the factors affecting accuracy of SUV measurements. AJR Am J Roentgenol. 2010;195(2):310–20.
27. Fendler WP, Philippe Tiega DB, Ilhan H, et al. Validation of several SUV-based parameters derived from 18F-FDG PET for prediction of survival after SIRT of hepatic metastases from colorectal cancer. J Nucl Med. 2013;54(8):1202–8.
28. Kostakoglu L, Chauvie S. Metabolic tumor volume metrics in lymphoma. Semin Nucl Med. 2018;48(1):50–66.
29. Kim TM, Paeng JC, Chun IK, et al. Total lesion glycolysis in positron emission tomography is a better predictor of outcome than the International Prognostic Index for patients with diffuse large B cell lymphoma. Cancer. 2013;119(6):1195–202.
30. Lin C, Bradshaw T, Perk T, et al. Repeatability of quantitative 18F-NaF PET: a multicenter study. J Nucl Med. 2016;57(12):1872–9.